Radial and longitudinal motion of the arterial wall: Their relation to pulsatile pressure and flow in the artery

Dan Wang,[1] Linda Vahala,[2] and Zhili Hao[1]
[1]*Department of Mechanical and Aerospace Engineering, Old Dominion University, Norfolk, Virginia 23529, USA*
[2]*Department of Electrical and Computer Engineering, Old Dominion University, Norfolk, Virginia 23529, USA*

(Received 21 March 2018; published 4 September 2018)

The aim of this paper is to analyze the radial and longitudinal motion of the arterial wall in the context of pulsatile pressure and flow, and to understand their physiological implications for the cardiovascular system. A reexamination of the well-established one-dimensional governing equations for axial blood flow in the artery and the constitutive equation for the radial dilation of the arterial wall shows that two waves—a pulsatile pressure wave in the artery and a radial displacement wave in the arterial wall—propagate simultaneously along the arterial tree with the same propagation velocity, explaining why this velocity combines the physical properties and geometries of both the blood and the arterial wall. With consideration of their coupling, the governing equations for the radial motion and longitudinal motion of the arterial wall are derived separately. The driving force for the radial motion of the arterial wall arises from its longitudinal motion. The longitudinal motion of the arterial wall is the standard longitudinal elastic wave with two driving forces: one associated with the pulsatile flow rate and the other associated with the radial motion. These derived governing equations shed insights on some recent experimental findings in the literature, including the correlation of measured arterial wall stiffness (solely based on the radial motion) to its longitudinal motion, the decreasing trend of arterial wall distensibility from the aorta to the periphery, the underlying mechanism of the longitudinal motion pattern of the common carotid arterial wall, and the motion pattern variation in longitudinal motion with aging and diseases.

DOI: 10.1103/PhysRevE.98.032402

I. INTRODUCTION

The motion of the arterial wall accompanies the pulsatile pressure and flow in the artery, and plays a critical role in blood circulation throughout the arterial tree [1–4]. Therefore, the motion of the arterial wall has been investigated for its clinical implications of cardiovascular diseases (CVDs) and vascular diseases [5–8]. As the main focus of extensive research, the radial motion of the arterial wall has formed the basis for estimation of the arterial wall stiffness, mostly in terms of pulse wave velocity (PWV), with the longitudinal motion being neglected [5,9]. Nowadays, PWV is a well-established independent risk predictor of adverse cardiovascular events. However, current established methods for measuring the arterial wall stiffness cannot discern small preclinical atherosclerotic or arteriosclerotic changes in a comprehensive manner [6]. Yet, detecting these preclinical aberrant changes in the arterial tree could be beneficial in developing novel strategies to prevent the progress of vascular diseases [6]. Compared with its radial motion, the longitudinal motion of the arterial wall has been suggested to be an earlier and more sensitive measure of vascular diseases [10,11]. Experimental studies have recently found that the measured arterial wall stiffness solely based on the radial motion is correlated to the longitudinal motion amplitude of the arterial wall [8,12,13]. For the purpose of devising new clinic indexes for detecting preclinical aberrant changes and finding its influence on the radial motion of the arterial wall, the longitudinal motion of the arterial wall needs to be studied.

Thanks to the advancement in imaging techniques over the past decade, the longitudinal motion of the arterial wall has been found to be of equal amplitude to the radial motion of the arterial wall [14]. The longitudinal motion of the arterial wall was investigated for the purpose of complementing the arterial wall stiffness based on the radial motion and developing new clinic indexes for vascular diseases [6,7,15,16]. Toward this end, several studies were conducted on finding the underlying mechanism of the longitudinal motion pattern of the arterial wall, but the conclusions from different studies are contradictory [13,15,17]. For instance, Ahlgren *et al.* [17] found that the wall shear stress (i.e., local blood flow) is not the main driving force of the longitudinal motion, while Au *et al.* [13] found that the local blood flow is closely related to the first anterograde motion of the longitudinal motion. These studies [13,15,17] investigated the longitudinal motion of the arterial wall purely from the physiological perspective (by altering one or two factors through drug administration and utilizing statistical analysis and/or machine learning to establish their correlation to the longitudinal motion). Yet, the determinants of the bidirectional pattern of the longitudinal motion of the arterial wall remain unclear [11,15], although new clinical indexes have been created from the measured longitudinal motion of the arterial wall via machine-learning techniques [16].

Since the pulsatile pressure and flow in the artery are adjacent to the arterial wall and accompany the motion of the arterial wall, intuitively, a direct relation should exist between these two parameters in the artery and the radial and longitudinal motion of the arterial wall. Then, the question arises: How are pulsatile pressure and flow related to the radial and longitudinal motion of the arterial wall? From the mechanical

perspective, this work derives the governing equations of the radial and longitudinal motion of the arterial wall, and analyzes how the radial (u_r) and longitudinal (u_x) motion of the arterial wall is related to the pulsatile pressure (Δp) and flow rate (Q) in the artery. Comparison of the analyzed results with some recent experimental findings in the literature [6,13,17] sheds insights on the physiological implications of the radial and longitudinal motion of the arterial wall to the cardiovascular system. As such, they may serve as the basis for developing model-based clinical indexes from the measured radial and longitudinal motion of the arterial wall for inferring the cardiovascular system condition, instead of machine-learning-based clinical indexes.

The rest of the paper is organized as follows. In Sec. II, without considering the longitudinal motion, the well-established one-dimensional (1D) governing equations for axial blood flow in the artery and the constitutive equation for the radial dilation of the arterial wall are reexamined for the role of the radial motion of the arterial wall in pulsatile pressure and flow in the artery. In Sec. III, by treating the arterial wall as a thin-walled tube and considering radial-longitudinal coupling in its motion, the governing equations for the radial motion and longitudinal motion of the arterial wall are derived separately. The physiological implications of the derived governing equations are discussed and utilized to explain some recent experimental findings in the literature in Sec. IV. The last section concludes the gained physiological implications of the radial and longitudinal motion of the arterial wall.

II. ROLE OF THE RADIAL MOTION OF THE ARTERIAL WALL IN PULSATILE PRESSURE AND FLOW IN THE ARTERY

A. Governing equations for axial blood flow in the artery and the radial motion of the arterial wall

The blood circulation in the arterial tree involves complex three-dimensional (3D) fluid-structure interaction between the blood flow in the artery and the motion of the arterial wall [18,19]. To better understand the physiological implications of the hemodynamic parameters and arterial wall motion parameters to cardiovascular diseases, 1D modeling of the blood flow in an artery has been well established and validated by experimental studies to some extent [1]. The fundamental assumptions underlying the 1D modeling are summarized below [1,19]:

(1) The artery has a straight, uniform, circular shape and entails axis-symmetric blood flow.

(2) The blood in the artery is an incompressible homogeneous Newtonian fluid.

(3) The density ρ_b and viscosity μ_b of the blood are constant.

(4) Small disturbances (i.e., arterial pulses) with the angular frequency ω and the wavelength λ take place in an artery with the radius being much smaller than the wavelength (i.e., $r_0 \ll \lambda$) and thus no blood flow along the radial direction occurs.

(5) As to large arteries (e.g., common carotid artery and aorta), the Womersley number $\alpha = r_0\sqrt{\rho_b\omega/\mu_b}$ is much larger than 1. Then, the boundary layer is thin and the blood flow velocity profile is close to plug flow. Therefore, the pressure and velocity are assumed to be uniform over the entire cross section.

As shown in Fig. 1, the 1D governing equations of axial pulsatile flow in a distensible artery are then derived from conservation of mass (equation of continuity) and conservation of momentum (Navier-Stokes equation) along the axial direction (x axis) of the artery [1]:

$$\frac{\partial A}{\partial t} + \frac{\partial (AU)}{\partial x} = 0, \tag{1a}$$

$$\frac{\partial U}{\partial t} + U\frac{\partial U}{\partial x} = -\frac{1}{\rho_b}\frac{\partial p}{\partial x} + \frac{f}{\rho_b A} \quad \text{(TA)} \quad \text{(CA)} \quad \text{(PG)} \quad \text{(VF)}, \tag{1b}$$

where $U(x, t)$ and $p(x, t)$ denote the blood flow velocity and blood pressure averaged over the entire cross section, respectively; $A(x, t)$ is the cross-section area of the lumen; and f denotes the friction force in the blood flow. The blood flow rate, $Q = AU$, is the product of the average blood flow velocity and the cross-section area. The terms in the Navier-Stokes equation are the temporal acceleration (TA), convective acceleration (CA), pressure gradient (PG), and the viscous force (VF). Given the small disturbances and the plug flow, the CA is negligible [1]. When the Womersley number is much larger than 1, the VF is also small, relative to the TA and the PG [1,19].

The above two equations contain three time-varying parameters: blood pressure (p), blood flow velocity (U), and cross-section area (A) of the artery, which varies with radial dilation of the arterial wall. To complement the above two equations, the constitutive equation of the arterial wall (or arterial wall compliance) [9] is included in Eq. (1a):

$$C_A = \frac{\partial A(t)}{\partial p(t)} = \frac{2\pi r_0 \partial u_r(t)}{\partial p(t)}, \tag{1c}$$

where $u_r(t)$ is the radial displacement of the arterial wall and r_0 is the artery radius at diastolic pressure P_d. Both r_0 and C_A are related to the transmural pressure in the arterial wall: $P_T = P_{\text{ext}} - P_d$, with P_{ext} being the pressure outside the arterial wall.

In Eq. (1c), a purely elastic, linear relation between the pulsatile pressure and the radial displacement is assumed for the arterial wall. Furthermore, the radial displacement amplitude, u_{r0}, is assumed to be much smaller than the arterial radius r_0 (i.e., $u_{r0}/r_0 \ll 1$). By taking the first-order derivative of Eq. (1c) with respect to t and x, respectively, the following relations between the radial displacement and the pulsatile pressure are obtained:

$$\frac{\partial p}{\partial t} = \frac{1}{C_A}\frac{\partial A}{\partial t} = \frac{2\pi r_0}{C_A}\frac{\partial u_r}{\partial t}, \tag{2a}$$

$$\frac{\partial p}{\partial x} = \frac{1}{C_A}\frac{\partial A}{\partial x} = \frac{2\pi r_0}{C_A}\frac{\partial u_r}{\partial x}. \tag{2b}$$

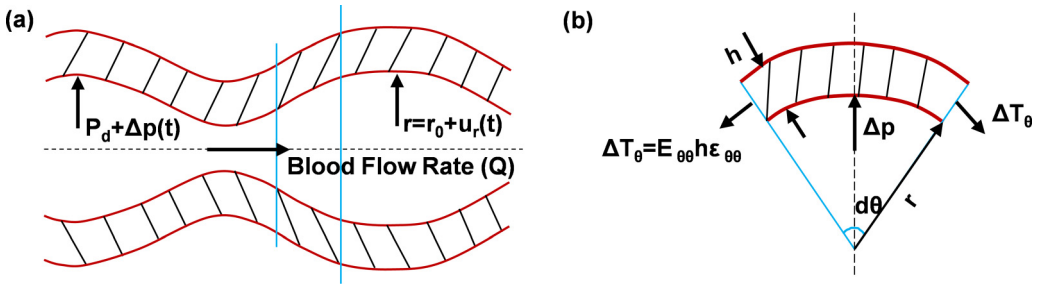

FIG. 1. Schematics of (a) pulsatile pressure $\Delta p(t)$ and axial blood flow Q in the artery and (b) circumferential tension force ΔT_θ in the arterial wall due to its radial dilation u_r.

B. Pulsatile pressure wave in the artery

Substituting Eq. (2a) into Eq. (1a) yields the following relation:

$$C_A\frac{\partial p}{\partial t}+\frac{\partial(AU)}{\partial x}=0. \tag{3}$$

Now, we take the derivative of Eq. (3) with respect to t and take the derivative of Eq. (1b) with respect to x, add up the two equations, and neglect the two small terms (CA and VF):

$$\frac{\partial^2 p}{\partial t^2}=\frac{A}{\rho_b C_A}\frac{\partial^2 p}{\partial x^2}. \tag{4}$$

Equation (4) indicates that there is a pulsatile pressure wave in the artery propagating along the arterial tree with the propagation velocity (v_P), commonly referred to as the pulse wave velocity:

$$v_P^2=\frac{A}{\rho_b C_A}. \tag{5}$$

By treating the arterial wall as a stretched thin-walled membrane in a circular shape with constant thickness h and constant density ρ_w, the radial displacement u_r gives rise to a circumferential tension force ΔT_θ, as shown in Fig. 1(b). This tension force can be expressed using an effective incremental circumferential modulus $E_{\theta\theta}$ of the arterial wall:

$$\Delta T_\theta=E_{\theta\theta}h\frac{u_r}{r_0}=r_0\Delta p. \tag{6}$$

Note that this circumferential tension force needs to counterbalance the radial force arising from the pulsatile pressure, Δp. Then, the arterial wall compliance is related to the physical properties and geometries of the arterial wall by

$$C_A=\frac{\partial A}{\partial p}=\frac{2r_0A_0}{E_{\theta\theta}h}. \tag{7}$$

Substituting Eq. (7) into Eq. (5) leads to the well-known Moens-Korteweg formula [5]:

$$v_P=\sqrt{\frac{E_{\theta\theta}h}{2r_0\rho_b}}. \tag{8}$$

C. Radial displacement wave in the arterial wall

Now, we derive the governing equation for the radial motion of the arterial wall by replacing the pulsatile pressure with the radial displacement in Eqs. (1a) and 1(b). Substituting Eq. (2b) into Eqs. (1a) and (1b) gives rise to the following two equations:

$$2\pi r_0\frac{\partial u_r}{\partial t}+\frac{\partial(AU)}{\partial x}=0, \tag{9a}$$

$$\frac{\partial U}{\partial t}+U\frac{\partial U}{\partial x}=-\frac{1}{\rho}\frac{2\pi r_0}{C_A}\frac{\partial u_r}{\partial x}+\frac{f}{\rho A}. \tag{9b}$$

By neglecting the two small terms (CA and VF) in Eq. (9b) and combining the above two equations, the governing equation for the radial motion of the arterial wall is obtained:

$$\frac{\partial^2 u_r}{\partial t^2}=\frac{A}{\rho_b C_A}\frac{\partial^2 u_r}{\partial x^2}. \tag{10}$$

Equation (10) indicates that there is a radial displacement wave in the arterial wall (similar to a transverse wave in a string) propagating along the arterial tree. Comparison of Eqs. (4) and (10) shows that the radial displacement wave in the arterial wall and the pulsatile pressure wave in the artery propagate simultaneously (Windkessel effect) along the arterial tree with the same propagation velocity. Mathematically, the coincidence of the two waves arises from the definition of the arterial wall compliance in Eq. (1c) and explains why the propagation velocity combines the physical properties and geometries of the blood and the arterial wall. The experimentally observed similarity between arterial radius waveform and pulsatile pressure waveform [20] is coined in the arterial wall compliance.

D. Driving force for the pulsatile flow in the artery

Based on Eqs. (1b) and (9b), the driving forces for the pulsatile flow velocity (U) or pulsatile flow rate (Q) in the artery include the pressure gradient $\partial p/\partial x$ and the radial displacement gradient, $\partial u_r/\partial x$. According to Eqs. (2b) and (7), the pressure gradient is related to the radial displacement gradient by

$$\frac{\partial p}{\partial x}=\frac{E_{\theta\theta}h}{r_0^2}\frac{\partial u_r}{\partial x}. \tag{11}$$

The pressure gradient is commonly related to the pulsatile flow rate Q by the vascular resistance R [21]:

$$Q=\frac{\partial p}{\partial x}\Big/R=\frac{E_{\theta\theta}h}{r_0^2R}\frac{\partial u_r}{\partial x}\frac{\partial u_r}{\partial x}\quad\text{with}\quad R=\frac{8L\mu_b}{\pi {r_0}^4}, \tag{12}$$

where L is the arterial length.

III. COUPLED RADIAL AND LONGITUDINAL MOTION OF THE ARTERIAL WALL

The arterial wall is treated as a stretched thin-walled membrane in a circular shape with constant thickness h and the constant density ρ_w. The wall thickness is much smaller than the wall radius, $h/r_0 \ll 1$. Figure 2 shows a small segment of angle $d\theta$ and length dx of the arterial wall, which is at the transmural pressure P_T, and is axially prestretched along its longitudinal direction. The circumferential and longitudinal tension forces in the arterial wall at diastolic pressure are $T_{0\theta}$ and T_{0x}, respectively. As such, the arterial wall is analogous to a stretched spring moving along both directions, whereas the arterial wall in Eqs. (1c) and (6) is treated as a stretched thin-walled membrane with a purely elastic, linear relation of the pulsatile pressure to the radial displacement, and undergoes only radial motion. The wall segment undergoes radial motion $u_r(t)$ and longitudinal motion $u_x(t)$ in a pulse cycle.

A. Radial motion of the arterial wall

The arterial wall segment in Fig. 2 is subject to the following forces along the radial direction:

(1) A radial force results from the pulsatile pressure:

$$F_{p-r} = \Delta p r_0 d\theta dx. \tag{13}$$

(2) The arterial wall experiences a circumferential strain: $\varepsilon_{\theta\theta} = u_r/r_0$. Then, the restoring force from the arterial wall along the radial direction becomes

$$F_{\theta-r} = -\left(E_{\theta\theta} h \varepsilon_{\theta\theta} d\theta dx + \eta_{\theta\theta} h \frac{d\varepsilon_{\theta\theta}}{dt} d\theta dx\right), \tag{14}$$

where the second term is the viscous term with $\eta_{\theta\theta}$ being the effective damping modulus of the arterial wall.

(3) Because of its radial motion, the arterial wall deforms along its longitudinal direction. The radial component from the longitudinal tension force of the wall segment is [22,23]

$$\Delta T_{x-r} = E_{xx} h r_0 d\theta \frac{\partial}{\partial x}\left\{\left[\frac{\partial u_x}{\partial x} + \frac{1}{2}\left(\frac{\partial u_r}{\partial x}\right)^2\right]\frac{\partial u_r}{\partial x}\right\} dx, \tag{15}$$

where E_{xx} is an effective incremental longitudinal modulus of the arterial wall. Since the second term is small relative to the first term in the square brackets, the overall radial component from the longitudinal tension force becomes

$$F_{x-r} = E_{xx} h r_0 d\theta \frac{\partial}{\partial x}\left(\frac{\partial u_x}{\partial x}\frac{\partial u_r}{\partial x}\right) dx. \tag{16}$$

According to Newton's second law, the governing equation of the radial motion of the arterial wall segment is

$$\rho_w h r_0 d\theta dx \frac{d^2 u_r}{dt^2} = F_{\theta-r} + F_{x-r} + F_{p-r}. \tag{17}$$

Substituting the expressions for the radial forces into Eq. (17) gives rise to

$$\frac{d^2 u_r}{dt^2} + \frac{E_{\theta\theta}}{\rho_w r_0^2} u_r + \frac{\eta_{\theta\theta}}{\rho_w r_0^2}\frac{du_r}{dt} = \frac{E_{xx}}{\rho_w}\frac{\partial}{\partial x}\left\{\frac{\partial u_x}{\partial x}\frac{\partial u_r}{\partial x}\right\} + \frac{\Delta p}{\rho_w h}. \tag{18}$$

When the time-variant terms in Eq. (18) are zero and the longitudinal motion term is neglected, the above equation reduces to Eq. (6) and consequently we have the arterial wall compliance:

$$\frac{E_{\theta\theta}}{\rho_w r_0^2} u_r = \frac{\Delta p}{\rho_w h} \rightarrow C_A = \frac{\Delta A}{\Delta p} = \frac{2 r_0 A_0}{E_{\theta\theta} h}. \tag{19}$$

As such, the measured arterial wall stiffness (v_P) in Eq. (8) ignores the viscous nature of the radial motion of the arterial wall and the influence of the longitudinal motion on the radial motion. After removing the inertial term and the longitudinal motion term, Eq. (18) becomes the commonly used Kelvin-Voigt material model for the arterial wall [4]:

$$\frac{E_{\theta\theta}}{\rho_w r_0^2} u_r + \frac{\eta_{\theta\theta}}{\rho_w r_0^2}\frac{du_r}{dt} = \frac{\Delta p}{\rho_w h}. \tag{20}$$

Based on this equation, the elasticity and viscosity of the arterial wall are currently extracted from simultaneously measured pulsatile pressure waveform and artery radius waveform at the same arterial location. Comparison of Eq. (20) with Eq. (18) indicates that while the driving force for the quasistatic radial motion is the pulsatile pressure, the dynamic radial motion (acceleration) of the arterial wall arises from the radial force component of the longitudinal motion of the arterial wall.

By replacing the pulsatile pressure with the radial displacement using Eq. (1c), Eq. (18) becomes

$$\frac{d^2 u_r}{dt^2} + \left(\frac{E_{\theta\theta}}{\rho_w r_0^2} - \frac{2\pi r_0}{C_A \rho_w h}\right) u_r + \frac{\eta_{\theta\theta}}{\rho_w r_0^2}\frac{du_r}{dt} = \frac{E_{xx}}{\rho_w}\frac{\partial}{\partial x}\left\{\frac{\partial u_x}{\partial x}\frac{\partial u_r}{\partial x}\right\}. \tag{21}$$

Accordingly, the arterial wall at any axial position behaves as a second-order dynamic system and undergoes radial vibrations, with the driving force from the longitudinal motion.

By replacing the radial displacement in Eq. (18) with the pulsatile pressure using Eq. (1c), the governing equation for the pulsatile pressure acting on the arterial wall is obtained:

$$\frac{d^2 \Delta p}{dt^2} + \left(\frac{E_{\theta\theta}}{\rho_w r_0^2} - \frac{2\pi r_0}{C_A \rho_w h}\right) \Delta p + \frac{\eta_{\theta\theta}}{\rho_w r_0^2}\frac{d\Delta p}{dt} = \frac{E_{xx} r_0^2}{E_{\theta\theta} \rho_w h}\frac{\partial}{\partial x}\left\{\frac{\partial u_x}{\partial x}\frac{\partial u_r}{\partial x}\right\}. \tag{22}$$

The pulsatile pressure variation on the arterial wall is caused by the radial force component of the longitudinal motion of the arterial wall. Comparison of Eq. (22) with Eq. (21) suggests that the pulsatile pressure acting on the arterial wall and the radial motion of the arterial wall accompany each other and exhibit the same dynamic nature. Taken together, locally at any axial position, the radial motion of the arterial wall and pulsatile pressure variation in the artery accompany each other and are both caused by the longitudinal motion of the arterial wall; systemically along the arterial tree, the radial displacement wave and pulsatile pressure wave propagation are driven by the pressure gradient and the radial displacement gradient.

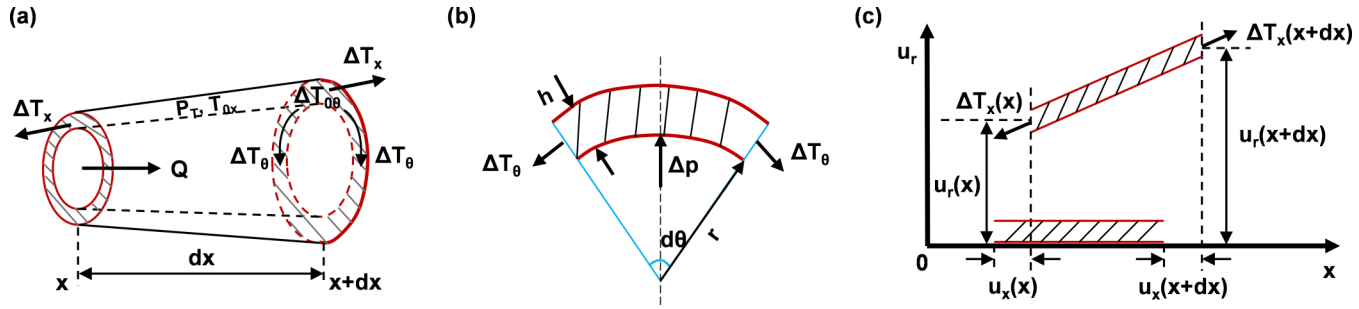

FIG. 2. Coupled radial motion (u_r) and longitudinal motion (u_x) of a small segment of angle $d\theta$ and length dx of the arterial wall. (a) A segment of artery of length dx. Q: the blood flow rate in the artery; P_T: the transmural pressure in the arterial wall; T_{0x}: the longitudinal tension force in the arterial wall at diastolic pressure; $T_{0\theta}$: the circumferential tension force in the arterial wall at diastolic pressure; ΔT_θ: the circumferential force due to the radial displacement. (b) Radial direction. h: arterial wall thickness; Δp: pulsatile pressure; $r = r_0 + u_r$: the arterial wall radius. (c) Longitudinal direction. $u_x(x)$ and $u_x(x + dx)$: longitudinal displacements at the positions of x and $x + dx$, respectively; $u_r(x)$ and $u_r(x + dx)$: radial displacements at the positions of x and $x + dx$, respectively.

B. Longitudinal motion of the arterial wall

The arterial wall segment in Fig. 2 is subject to the following forces along the longitudinal direction:

(1) The longitudinal motion of the arterial wall gives rise to the overall tension force:

$$F_{x-x} = E_{xx} h r_0 d\theta \frac{\partial^2 u_x}{\partial x^2} dx. \tag{23}$$

(2) Owing to the radial motion of the arterial wall, the pulsatile pressure results in a longitudinal force:

$$F_{p-x} = -\Delta p \frac{\partial u_r}{\partial x} r_0 d\theta dx = -\frac{2\pi r_0}{C_A} u_r \frac{\partial u_r}{\partial x} r_0 d\theta dx. \tag{24}$$

Note that the pulsatile pressure is further expressed in terms of the radial displacement.

(3) The blood flow rate causes the wall shear stress τ_w on the arterial wall. The overall shear force caused by the blood flow rate becomes [20]

$$F_{Q-x} = \tau_w r_0 d\theta dx = \frac{4\eta_b Q}{\pi r_0^3} r_0 d\theta dx. \tag{25}$$

By summarizing the above equations, the governing equation for the longitudinal motion of the arterial wall becomes

$$\frac{d^2 u_x}{dt^2} = \frac{E_{xx}}{\rho_w} \frac{\partial^2 u_x}{\partial x^2} - \frac{\pi E_{\theta\theta}}{A_0 \rho_w} u_r \frac{\partial u_r}{\partial x} + \frac{4\eta_b Q}{\rho_w \pi r_0^3 h}, \tag{26a}$$

$$\frac{d^2 u_x}{dt^2} = \frac{E_{xx}}{\rho_w} \frac{\partial^2 u_x}{\partial x^2} - \frac{\Delta p}{h \rho_w} \frac{\partial u_r}{\partial x} + \frac{4\eta_b Q}{\rho_w \pi r_0^3 h}. \tag{26b}$$

Equation (26) indicates that there is a longitudinal elastic wave in the arterial wall propagating along the arterial tree, with the propagation velocity solely related to the physical properties of the arterial wall. There are two driving forces for the longitudinal motion: one associated with the radial motion (or pulsatile pressure) and the other associated with the blood flow rate. The force associated with the blood flow rate is in the opposite direction to the force associated with the radial motion. Thus, a high blood flow rate may cause a large longitudinal motion, but the force associated with the radial motion counteracts the force associated with the blood flow rate to reduce the longitudinal motion amplitude.

IV. DISCUSSION

A. Correlation of the longitudinal motion of the arterial wall to the radial motion of the arterial wall

Taivainen *et al.* [8] recently found that the longitudinal motion amplitude of the common carotid wall were directly correlated with its distensibility and inversely correlated with its PWV. Based on Eq. (21), the driving force for the radial motion is the longitudinal motion. Then, high longitudinal motion amplitude translates to high distensibility. As explained below, high distensibility indicates low circumferential modulus and thus is accompanied with low PWV, according to Eq. (8).

Elastic arteries are significantly prestretched along their axial (longitudinal) direction, setting up their tension state (T_{0r} and $T_{0\theta}$) at diastolic pressure. With this axial prestretch, the radial motion of the arterial wall and the pulsatile pressure variation happen at any axial position, and enable the propagation of the radial displacement wave and the pulsatile pressure wave along the arterial tree. It was found [24] that high axial prestretch (or high longitudinal modulus E_{xx}) translates to a large radial motion and thus a high distensibility, which is possibly due to the axial prestretch aligning collagen fibers to the axial direction, then leading to a low circumferential modulus ($E_{\theta\theta}$). According to Eq. (21), the combination of high longitudinal modulus and low circumferential modulus translates to high distensibility. Conversely, low axial prestretch corresponds to low longitudinal modulus and high circumferential modulus. Furthermore, given the same mean blood pressure, a highly axially prestretched arterial wall can exhibit higher distensibility than a less axially prestretched arterial wall [24]. Since a change in axial prestretch is typically accompanied by changes in artery radius and mean blood pressure, all these factors adjust the circumferential and longitudinal modulus of the arterial wall, and consequently its radial and longitudinal motion.

As the arterial wall stiffness increases from the aorta to the periphery [25], axial prestretch and artery radius decrease with more distal arterial locations [26]. Low axial prestretch

in a peripheral artery translates to a low longitudinal modulus and a high circumferential modulus. Based on Eq. (21), the driving force for the radial motion is reduced, but the stiffness in the radial motion, which is proportional to the ratio of the circumferential modulus to the squared artery radius, is increased. Consequently, Eq. (21) explains the reason that the arterial wall distensibility decreases from the aorta to the periphery [25,26]. Based on Eq. (22), the pulsatile pressure amplitude increases from the aorta to the periphery, because of the accompanying increased ratio of longitudinal modulus to circumferential modulus.

B. Bidirectional pattern of the longitudinal motion of the common carotid arterial wall in healthy young subjects

Most of the studies on the longitudinal motion focused on the common carotid artery, due to its easy access. This artery has been shown to undergo a multiphasic bidirectional motion pattern in healthy young subjects: an anterograde motion (in the direction of the blood flow) in early systole, a retrograde motion (in the direction of opposing blood flow) in late systole, and then a second distinct anterograde-retrograde motion with a lower amplitude in diastole than the one in systole [14,27]. The study conducted by Cinthio *et al.* [14] demonstrated that the first anterograde motion peak occurs after the blood flow rate peak but before the radial motion peak. Thus, the blood flow rate in Eq. (26) is the dominant driving force for the longitudinal motion of the arterial wall. After the blood flow rate recedes significantly and the first anterograde motion peak is reached in systole, the longitudinal restoring tension in the arterial wall starts to drive the arterial wall into its first retrograde motion in late systole. According to Au *et al.* [13], the first retrograde motion is associated with left ventricle rotation and thus an active regulatory factor may also contribute to this retrograde motion in late systole. This factor also explains why the first retrograde motion has a relatively large amplitude, as compared with the first anterograde motion.

With the aid of a low late systolic blood flow rate peak, the longitudinal restoring tension moves the arterial wall into the second anterograde-retrograde motion in diastole. Based on Eq. (21), the radial motion of the arterial wall should register the second anterograde-retrograde motion. The end of the first retrograde motion occurs almost simultaneously with the dicrotic notch in the radial motion [14,17], indicating that the radial motion does capture the second anterograde-retrograde motion, but with a much smaller amplitude. This is possibly due to the active regulatory factor from the left ventricle existing only in the longitudinal motion, but not in the radial motion.

To investigate the underlying mechanism of the longitudinal motion of the carotid arterial wall, Ahlgren *et al.* [28] altered certain hemodynamic parameters in anesthetized pigs by administration of catecholamines and found that the longitudinal motion of the carotid wall undergoes profound change in response to catecholamine. By administration of epinephrine, norepinephrine, and β-blockade (metoprolol) in anesthetized pigs, Ahlgren *et al.* [17] found that the longitudinal motion of the carotid arterial wall has no correlation with the blood flow rate. However, when the blood flow rate was altered, many interdependent factors, including the radius, distensibility, and circumferential and longitudinal modulus of the carotid arterial wall, were also altered by catecholamine administration. As shown in Eq. (26), the longitudinal motion of the arterial wall is a collective effort of all these interdependent factors. Later on, Au *et al.* [15] investigated the influence of some physiological factors on the longitudinal motion of the carotid arterial wall in young healthy human subjects through sympathetic activation and vascular smooth muscle relaxation. This study also could not establish significant correlation of the blood flow rate to the first anterograde motion in early systole by vascular smooth muscle relaxation. Similarly, the vascular smooth muscle relaxation alters not only the blood flow rate, but also other interdependent factors. Moreover, since administration of different drugs alters regulatory control over the arterial tree, the axial prestretch in the arterial wall might also be altered. It has been found that the axial prestretch is not negligible in mechanobiological processes, including its adaptation response to elevated blood pressure [29]. The axial prestretch dictates the tension state of the arterial wall at diastolic pressure and thus determines wall thickness, radius, and the circumferential and longitudinal modulus. As such, the studies on the underlying mechanism of the longitudinal motion of the arterial wall via drug administration should take these interdependent factors into account.

C. Motion pattern variation of the longitudinal motion of the common carotid arterial wall with aging and diseases

The longitudinal motion pattern of the carotid arterial wall was found to vary with aging [27]. Different from its counterpart in young healthy subjects, the longitudinal motion pattern of the common carotid artery in middle-aged and older subjects were found to include the appearance of two additional distinct phases of motion [27]. Both the axial prestretch and the distensibility are found to decline with aging [24]. The low longitudinal tension (T_{0x}) at diastolic pressure due to decreased axial prestretch goes down to a larger extent than the circumferential tension ($T_{0\theta}$) at diastolic pressure. The low longitudinal tension translates to a low longitudinal modulus (E_{xx}). At the same time, a late systolic flow velocity peak exists in the carotid flow velocity waveform and increases with aging. Heffernan *et al.* [30] found that both increased pressure from wave reflections and increased suction from the left ventricle contribute to the late systolic flow augmentation. As such, it is the combination of the increased late systolic flow velocity peak and the much decreased longitudinal modulus that drives the arterial wall to bounce forward and backward in diastole along the longitudinal direction.

The longitudinal motion pattern of the carotid arterial wall was also found to vary with diseases. Tat *et al.* [31] found that the presence of carotid plaque can have significant influence on the longitudinal motion of the arterial wall, with significantly greater anterograde motion amplitude with increased stenosis. Stenosis reduces the artery radius and increases the blood flow rate. According to Eq. (26), the dominant driving force for the longitudinal motion of the carotid arterial wall is significantly increased by stenosis. On the other hand, the same group of authors [11] found that, as compared with their healthy counterparts, the first retrograde motion amplitude is

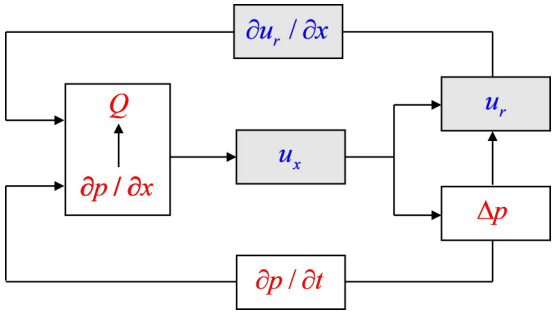

FIG. 3. Cause-effect relation of the radial and longitudinal motion (in blue) of the carotid arterial wall to the hemodynamic parameters (in red) in the common carotid artery, with the arrow showing the cause-effect direction.

much reduced but the first anterograde motion in the common carotid artery does not show a difference in subjects with spinal cord injury. Similar to the study conducted by Au *et al.* [13], the reduced first retrograde motion amplitude was attributed to left ventricle rotation in systole, which could produce the retrograde motion [11].

D. Timing of hemodynamic parameters in the artery and the radial and longitudinal motion of the common carotid arterial wall

Figure 3 shows the correlation of the hemodynamic parameters in the common carotid artery: pressure gradient, pulsatile pressure, and the blood flow rate to the radial and longitudinal motion of the arterial wall. According to Eq. (11), the blood flow rate and the pressure gradient accompany each other and thus are treated as two interdependent parameters. Similarly, the radial displacement wave in the arterial wall is accompanied by the pulsatile pressure wave in the artery and they are treated as two interdependent parameters too. Propagating in two different media (blood versus arterial wall), the radial displacement wave and the pulsatile pressure wave are separated in the figure.

According to the literature [32], the pressure gradient peak occurs before the flow rate peak, with the latter occurring before the pulsatile pressure peak: $\partial p/\partial x \rightarrow Q \rightarrow \Delta p$, indicating that the pressure gradient causes the blood flow rate and then the pulsatile pressure. According to Cinthio *et al.* [14], the blood flow rate peak occurs before the first anterograde motion peak of the carotid arterial wall: $Q \rightarrow u_x$. Since the radial motion of the arterial wall and the pulsatile pressure are both caused by the longitudinal motion, the longitudinal motion peak of the arterial wall should occur before the radial motion peak and the pulsatile pressure peak: $u_x \rightarrow \Delta p$ and $u_x \rightarrow u_r$. Two experimental studies [14,27] observed $u_x \rightarrow u_r$ at the carotid arterial wall. The relation of $\Delta p \rightarrow u_r$ has been validated by many experimental studies [4]. However, the experimental validation of $u_x \rightarrow \Delta p$ cannot be found in the literature. Nonetheless, the peaks of these five parameters for the carotid arterial wall should follow the following time sequence:

$$\partial p/\partial x \rightarrow Q \rightarrow u_x \rightarrow \Delta p \rightarrow u_r. \tag{27}$$

Equation (27) indicates that the pressure gradient causes the blood flow rate and then the longitudinal motion, which further causes the pulsatile pressure and then the radial motion.

Based on Eq. (9b), the radial displacement gradient causes the blood flow rate. The rate of pulsatile pressure variation drives the pressure gradient [32]:

$$\frac{\partial p}{\partial x} = -\frac{1}{v_P}\frac{\partial p}{\partial t}. \tag{28}$$

As such, a closed-loop cause-effect relation exists among the radial and longitudinal motion of the arterial wall and the hemodynamic parameters in the common carotid artery.

E. Limitations of the study

There are two major limitations of this study. One is the assumption that the arterial wall at any axial position is homogeneous along the circumferential and longitudinal directions. The other is the assumption that the arterial wall is a passive material and is not controlled by regulatory factors in a pulse cycle, except that left ventricle rotation is added to explain the large retrograde motion in late systole. Nevertheless, the derived governing equations for the arterial wall motion are helpful in shedding insights on some recent experimental findings in the literature and might aid in developing model-based clinical indexes for detection and early diagnosis of CVDs and vascular pathologies.

V. CONCLUSION

In this study, we have reexamined the 1D governing equations of axial blood flow in the artery and the constitutive equation of the arterial wall, derived the governing equations for the radial and longitudinal motion of the arterial wall with consideration of their coupling, and utilized the derived governing equations to explain some recent experimental findings in the literature. The comparison of the derived governing equations with the experimental findings in the literature gives rise to the following physiological implications of the radial and longitudinal motion of the arterial wall to the cardiovascular system:

(1) A pulsatile pressure wave in the artery and a radial displacement wave in the arterial wall simultaneously propagate along the arterial tree with the same propagation velocity, which is determined by the physical properties and geometries of the blood and the arterial wall.

(2) The radial motion of the arterial wall and the pulsatile pressure variation in the artery arise from the radial force component of the longitudinal motion of the arterial wall, establishing the correlation of the measured arterial wall distensibility with the longitudinal motion amplitude and explaining the decreasing trend of the arterial wall stiffness and the increasing trend of pulsatile pressure amplitude from the aorta to the periphery.

(3) The longitudinal motion of the common carotid arterial wall is primarily driven by the blood flow rate in the

common carotid artery and is also regulated by left ventricle rotation.

(4) The motion pattern variation of the longitudinal motion of the common carotid arterial wall with aging and diseases arises from changes in both the blood flow rate pattern and the interindependent factors associated with the arterial wall itself.

In the future, a scaling analysis of the terms in the derived governing equations and experimental studies are needed to validate the above conclusions.

[1] M. Willemet and J. Alastruey, Ann. Biomed. Eng. **43**, 190 (2015).
[2] G. Baltgaile, Perspect. Med. **1**, 146 (2012).
[3] D. Bia, I. Aguirre, Y. Zócalo, L. Devera, E. C. Fischer, and R. Armentano, Rev. Espań. Cardiol. (Engl. Ed.) **58**, 167 (2005).
[4] R. K. Warriner, K. W. Johnston, and R. S. Cobbold, Physiol. Meas. **29**, 157 (2008).
[5] T. Pereira, C. Correia, and J. Cardoso, J. Med. Biol. Eng. **35**, 555 (2015).
[6] H. Yli-Ollila, T. Laitinen, M. Weckström, and T. M. Laitinen, Clin. Physiol. Funct. Imaging **36**, 376 (2016).
[7] S. H. Taivainen, H. Yli-Ollila, M. Juonala, M. Kähönen, O. T. Raitakari, T. M. Laitinen, and T. P. Laitinen, Atherosclerosis **272**, 54 (2018).
[8] S. H. Taivainen, H. Yli-Ollila, M. Juonala, M. Kähönen, O. T. Raitakari, T. M. Laitinen, and T. P. Laitinen, Clin. Physiol. Funct. Imaging **37**, 305 (2017).
[9] C. Leguy, E. Bosboom, H. Gelderblom, A. Hoeks, and F. Van De Vosse, Med. Eng. Phys. **32**, 957 (2010).
[10] S. Svedlund and L. M. Gan, Clin. Physiol. Funct. Imaging **31**, 32 (2011).
[11] J. Tat, J. S. Au, P. J. Keir, and M. J. MacDonald, Clin. Physiol. Funct. Imaging **37**, 106 (2017).
[12] H. Yli-Ollila, M. P. Tarvainen, T. P. Laitinen, and T. M. Laitinen, Ultrasound Med. Biol. **42**, 2873 (2016).
[13] J. S. Au, D. S. Ditor, M. J. MacDonald, and E. J. Stöhr, Physiol. Rep. **4**, e12872 (2016).
[14] M. Cinthio, A. R. Ahlgren, J. Bergkvist, T. Jansson, H. W. Persson, and K. Lindstrom, Am. J. Physiol. Heart Circ. Physiol. **291**, H394 (2006).
[15] J. S. Au, P. A. Bochnak, S. E. Valentino, J. L. Cheng, E. J. Stöhr, and M. J. MacDonald, Exp. Physiol. **103**, 141 (2018).
[16] S. Qorchi, G. Zahnd, D. Galbrun, A. Sérusclat, P. Moulin, D. Vray, and M. Orkisz, IRBM **38**, 219 (2017).
[17] Å. R. Ahlgren *et al.*, Ultrasound Med. Biol. **41**, 1342 (2015).
[18] J. R. Womersley, Philos. Mag. **46**, 199 (1955).
[19] G. Morgan and J. Kiely, J. Acoust. Soc. Am. **26**, 323 (1954).
[20] D. Hughes, L. A. Geddes, J. D. Bourland, and C. F. Babbs, in *Acoustical Imaging*, edited by A. F. Metherell, Acoustical Imaging Book Series, Vol. 8 (Springer, Boston, MA, 1980), pp. 699–707.
[21] T. G. Papaioannou and C. Stefanadis, Hell. J. Cardiol. **46**, 9 (2005).
[22] N. Etchenique, S. R. Collin, and T. R. Moore, J. Acoust. Soc. Am. **137**, 1766 (2015).
[23] B. Bank and L. Sujbert, J. Acoust. Soc. Am. **117**, 2268 (2005).
[24] L. Horný, M. Netušil, and T. Voňavková, Biomech. Model. Mechanobiol. **13**, 783 (2014).
[25] C. Fortier and M. Agharazii, Pulse **3**, 159 (2015).
[26] A. V. Kamenskiy, I. I. Pipinos, Y. A. Dzenis, C. S. Lomneth, S. A. J. Kazmi, N. Y. Phillips, and J. N. MacTaggart, Acta Biomater. **10**, 1301 (2014).
[27] J. Albinsson, Advancements of 2D speckle tracking of arterial wall movements, Ph.D. thesis, Lund University, 2017.
[28] Å. R. Ahlgren, M. Cinthio, S. Steen, T. Nilsson, T. Sjöberg, H. W. Persson, and K. Lindström, Am. J. Physiol. Heart Circ. Physiol. **302**, H1102 (2011).
[29] L. Horný, T. Adámek, and M. Kulvajtová, Biomech. Model. Mechanobiol. **16**, 375 (2017).
[30] K. S. Heffernan, W. K. Lefferts, and J. A. Augustine, Int. J. Hypertens. **2013**, 920605 (2013).
[31] J. Tat, I. N. Psaromiligkos, and S. S. Daskalopoulou, Ultrasound Med. Biol. **42**, 2114 (2016).
[32] D. McDonald, J. Physiol. **127**, 533 (1955).